Modeling of HPA and HPA Linearization Through a Predistorter:

Global Broadcasting Service Applications

Tien M. Nguyen, James Yoh,
Andrew S. Parker, Diana M. Johnson,
The Aerospace Corporation
El Segundo, California

Hien T. Tran
North Carolina State University
Raleigh, North Carolina

Abstract

This paper presents a technique to linearize the High Power Amplifier (HPA) through a Predistorter (PD). The characteristics of the PD circuit is derived based on the extension of Saleh's model for HPA and a simple linear-log model. Numerical results will be shown for the Global Broadcasting Service (GBS) applications.

1. Introduction

The effects of AM-to-AM (amplitude distortion) and AM-to-PM (phase distortion) conversions caused by HPA amplifiers, such as Solid-State Power Amplifiers (SSPA) or Travelling Wave Tube Amplifiers (TWTA), are one of the major concerns to communication systems engineers [1-4]. These effects can cause intermodulation (IM) components and spectral regrowth, which are undesirable to system designs. The intermodulation components and the spectral regrowth can cause adjacent channel interference to other services. Furthermore, these effects also cause loss in power transmission. In addition, the effects of AM-AM and AM-PM can also cause the signal distortion that can degrade the Bit Error Rate (BER) performance.

When the baseband signal of a constant envelope QPSK signal is filtered, the resultant modulated QPSK signal no longer has the constant-envelop property. If the filtered QPSK signal is then passed through an HPA operating at saturation, the spectral regrowth is present at the output of the HPA. Similarly, when two constant envelop signals are combined and then passed through a power amplifier operating at saturation, the properties related to spectral regrowth and IM products become uncertain. In recent work [5], it has been shown that the spectral regrowth and power loss in the IM products can cause severe BER degradation. In order to reduce spectral regrowth and BER degradation associated with HPAs operating at saturation, an HPA linearizer is needed.

This paper investigates techniques for the linearization of an HPA to mitigate the AM-to-AM and AM-to-PM effects in digital communications systems. The proposed techniques presented in this paper are simple to implement with minimal cost. These techniques use a PD circuit to compensate for the AM-AM and AM-PM effects.

The material contained in this paper is organized as follows: Section 2 presents the mathematical modeling for the HPA and PD; Section 3 discusses the implementation of the proposed PD in Signal Processing Workstation (SPW) software; Section 4 applies the proposed techniques to GBS while Section 5 shows the numerical results for GBS applications. Finally Section 6 presents our main conclusions. The Appendix derives the linear-Log model.

2. Mathematical Modeling

Figure 1(a) shows a proposed implementation of the linearizer using the PD at baseband. This section describes the mathematical modeling for the HPA and PD circuits.

Figure 1(a). Proposed Implementation of the Linearizer Using PD at Baseband

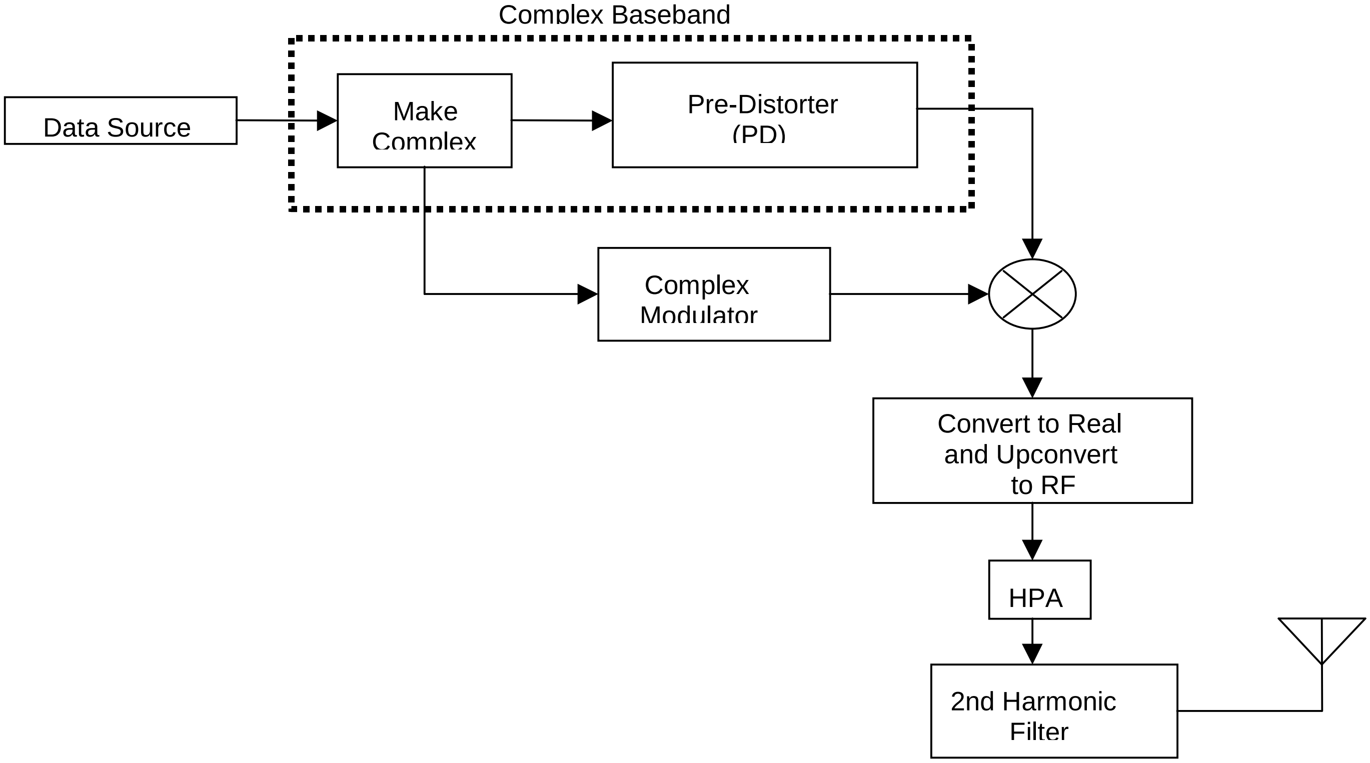

2.1 HPA Modeling

Based on Figure 1(a), Figure 1(b) shows a simplified block diagram for the HPA with a PD circuit.

Let X(t) be the input signal to the Predistorter (PD), Y(t) be the output of the PD and Z(t) be the output of the HPA amplifier. The complex baseband representations for these signals are:

$$X(t) = \rho_{x(t)} e^{j\theta_{x(t)}} \tag{1a}$$

$$Y(t) = \rho_{y(t)} e^{j\theta_{y(t)}} \tag{1b}$$

$$Z(t) = \rho_{Z(t)} e^{j\theta_{z(t)}} \tag{1c}$$

where $\rho_{x(t)}$, $\rho_{y(t)}$, $\rho_{z(t)}$, and $\theta_{x(t)}$, $\theta_{y(t)}$, $\theta_{z(t)}$ are the amplitude and phase of the complex signals X(t), Y(t) and Z(t), respectively.

If we let $M(\rho_{y(t)})$ and $\Phi(\rho_{y(t)})$ be the normalized AM-AM and AM-PM responses of the HPA due to the input signal Y(t), then Eqn (1c) becomes

$$Z(t) = M(\rho_{y(t)}) e^{j(\theta_{y(t)} + \Phi(\rho_{y(t)}))} \tag{2}$$

We extend Saleh's model [1] for HPA by including four extra parameters (a_0, a_1, b_0, and b_1), resulting in the following generalized equations for $M(\rho_{y(t)})$ and $\Phi(\rho_{y(t)})$:

$$M(\rho_{y(t)}) \equiv \rho_{Z(t)} = \frac{\alpha_0 \rho_{y(t)}}{a_0 + \beta_0 (\rho_{y(t)} + b_0)^2} \tag{3a}$$

$$\Phi(\rho_{y(t)}) = \frac{\alpha_1 \rho^2_{y(t)}}{a_1 + \beta_1 (\rho_{y(t)} + b_1)^2} \tag{3b}$$

Figure 1(b). Simplified Block Diagram for the Linearizer Using Predistorter Circuit

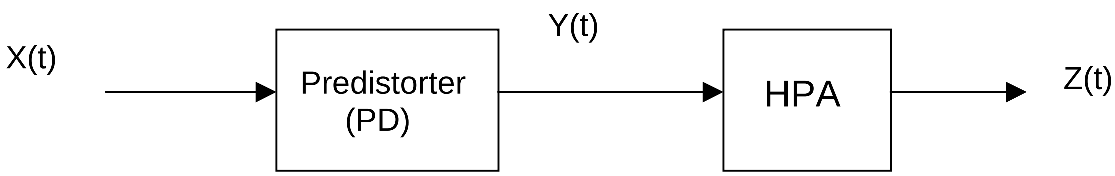

The unknown coefficients a_0, a_1, b_0, b_1, α_0, α_1, β_0 and β_1 are computed to give the best fit of the parameter-dependent Eqns (3a) and (3b) to the measured data. We refer the reader to the Appendix I for a description of the parameter estimation problem and the algorithm used to obtain its solution.

Note that from Eqn (1b) we can write $\exp(j\theta_{y(t)})$ as:

$$e^{j\theta_{y(t)}} = \frac{y(t)}{\rho_{y(t)}} \tag{4}$$

Substituting Eqns (4), (3a) and (3b) into Eqn (2) we obtain

$$Z(t) = \left[\frac{\alpha_0 Y(t)}{a_0 + \beta_0(\rho_{y(t)} + b_0)^2}\right] e^{j\left[\frac{\alpha_1 \cdot \rho^2_{y(t)}}{a_1 + \beta_1(\rho_{y(t)} + b_1)^2}\right]} \tag{5}$$

From Eqn (5), it is obvious that the ideal PD output for a given input X(t), is:

$$Y(t) = X(t)\left[\frac{a_0 + \beta_0(\rho_{y(t)} + b_0)^2}{\alpha_0}\right] e^{-j\left[\frac{\alpha_1 \cdot \rho^2_{y(t)}}{a_1 + \beta_1(\rho_{y(t)} + b_1)^2}\right]} \tag{6}$$

In the next section the PD algorithm will be derived from these basic equations, namely, Eqns (5) and (6).

2.2 PD Modeling

This section presents two techniques for modeling the PD. The first technique is based on Eqn (6), which is an extension of Saleh's model. The second model is based on a simple linear-log model.

2.2.1 Extended Saleh's Model

The amplitude and phase of the PD can be derived directly from Eqn (6). Substituting Eqn (1a) into Eqn (6), the amplitude and phase of the signal at the output of PD are:

$$\rho_{y(t)} = \left[\frac{a_0 + \beta_0(\rho_{y(t)} + b_0)^2}{\alpha_0}\right] \cdot \rho_{x(t)} \tag{7}$$

$$\theta_{y(t)} = \theta_{x(t)} - \left[\frac{\alpha_1 \cdot \rho^2_{y(t)}}{a_1 + \beta_1(\rho_{y(t)} + b_1)^2}\right] \tag{8}$$

It should be mentioned that the AM-AM relationship shown in Eqn (7) is usually expressed in terms of normalized input and output voltages or normalized input and output power.

Solving for $\rho_{y(t)}$ from Eqn (7) and selecting only the negative sign for the square-root term in the numerator, we have:

$$\rho_{y(t)} = \frac{\left[\alpha_0 - 2b_0\beta_0\rho_{x(t)}\right] - \sqrt{\alpha_0^2 - 4\beta_0\rho_{x(t)} \cdot \left[a_0\rho_{x(t)} + b_0\alpha_0\right]}}{2\beta_0\rho_{x(t)}} \tag{9}$$

Note that because of the normalized input and output relationship, the negative sign is chosen to meet the dual conditions that the square root term is real and $0 \le \rho_{y(t)} \le 1$.

If we let the amplitude and phase of the ideal PD be ρ_{PD} and θ_{PD}, respectively, then the output y(t) of the PD can be rewritten as:

$$Y(t) = X(t)\rho_{PD} e^{j\theta_{PD}} = \rho_{x(t)}\rho_{PD} e^{j(\theta_{x(t)} + \theta_{PD})} = \rho_{y(t)} e^{j\theta_{y(t)}} \tag{10}$$

Substituting Eqns (8) and (9) into Eqn (10) and equating the amplitude and phase terms separately for the ideal PD we obtain

$$\rho_{PD} = \frac{\rho_{y(t)}}{\rho_{x(t)}} = \begin{cases} \dfrac{\left[\alpha_0 - 2b_0\beta_0\rho_{x(t)}\right] - \sqrt{\alpha_0^2 - 4\beta_0\rho_{x(t)}\cdot\left[a_0\rho_{x(t)} + b_0\alpha_0\right]}}{2\beta_0\rho_{x(t)}^2}, & \rho_{x(t)} \le 1 \\ 1, & \rho_{x(t)} > 1 \end{cases} \quad (11)$$

$$\theta_{PD} = -\left[\frac{\alpha_1 \cdot \rho^2 y(t)}{a_1 + \beta_1(\rho_{y(t)} + b_1)^2}\right] \quad (12)$$

Note that the saturation condition for HPA is implied in Eqn (11).

Using the curve-fitting parameters (see Appendix I) we can implement Eqns (11) and (12) in an AM-AM and AM-PM look-up table or closed-form AM-AM and AM-PM expressions.

2.2.2 Linear-Log Model

In this model, we start with the two sets of measured data for the HPA, namely, the AM-AM curve of normalized input power and normalized output power, both of which being expressed in dB, and the AM-PM curve of normalized input power and output phase, expressed in dB and degree, respectively. From these two curves, we generate the corresponding AM-AM and AM-PM curves for the PD such that the combination of HPA and PD results in a X(t) and Z(t) being equal. The characteristics of the PD curves can be defined as (see Appendix II for the derivation):

$$P_{PD}(dB) = P_{IN}(dB) - P_{outHPA}(dB) \quad (13)$$

$$\theta_{PD}(degree) = -\,\theta_{HPA}(degree) \quad (14)$$

where $P_{IN}(dB)$ is the normalized input power to the AM-AM and AM-PM curves for both PD and HPA, $P_{PD}(dB)$ and $P_{outHPA}(dB)$ are the normalized output power from the AM-AM curves for PD and HPA, and $\theta_{PD}(degree)$ and $\theta_{HPA}(degree)$ are the output phases from the AM-PM curves for PD and HPA. The effect of HPA saturation at 0 dB is modeled by the following modification to Eqn (13):

$$P_{PD}(dB) = -\,P_{outHPA}(dB) \quad \text{for } P_{IN}(dB) > 0 \text{ dB} \quad (15)$$

Eqns (13) and (15) essentially stipulate that $P_{IN}(dB)$ can never be greater than 0 dB, the HPA input saturation level.

Using these characteristics, the complex signal Z(t) at the output of the HPA is identical to X(t). In other words, the input amplitude is directly proportional to the output amplitude without phase distortion, i.e.,

$$\rho_{z(t)} = \rho_{x(t)} \quad (16)$$

The AM-AM/AM-PM look-up table for the PD, using this approach, simply involves the $P_{IN}(dB)$ versus $P_{PD}(dB)$ curve for AM-AM and the $P_{IN}(dB)$ versus $\theta_{PD}(degree)$ curve for AM-PM.

2.2.3 Modified Linear-log Model

In the linear-log model described in Section 2.2.2, the composite AM-AM curve for the combination of PD and HPA is normalized in the sense that the input power and output power are both 0 dB at saturation. In the modified linear-log model, the composite AM-AM curve has a slightly smaller slope below saturation. This results in the output power being less than 0 dB (by Δ dB) at the input power of 0 dB. In other words, at the input saturation power of 0 dB this PD causes a loss of Δ dB at the HPA's output. In this model we also start with two sets of measured data: the AM-AM curve and AM-PM curve for the HPA. The characteristics of the PD curves can be defined as:

$$P_{PD\text{-}MOD}(dB) = Slope * P_{IN}(dB) - \Delta(dB) - P_{outHPA}(dB) \quad (17)$$

$$\theta_{PD\text{-}MOD}(degree) = -\,\theta_{HPA}(degree) \quad (18)$$

where Slope is given by:

$$Slope = [|P_{inHPA\text{-}min}(dB)| - |\Delta(dB)|] / |P_{inHPA\text{-}min}(dB)| \quad (19)$$

where $P_{inHPA\text{-}min}(dB)$ is the minimum normalized input power from the measured AM–AM curve for the HPA. The linear region ends at the input power of $\Delta(dB)/Slope$. Therefore, Eqn (17) must be modified by:

$$P_{PD\text{-}MOD}(dB) = -\,P_{outHPA}(dB) \quad \text{for } P_{IN}(dB) > \Delta(dB)/Slope \quad (20)$$

Figure 1(c). Simplified Block Diagram for the Implementation of the Linearizer

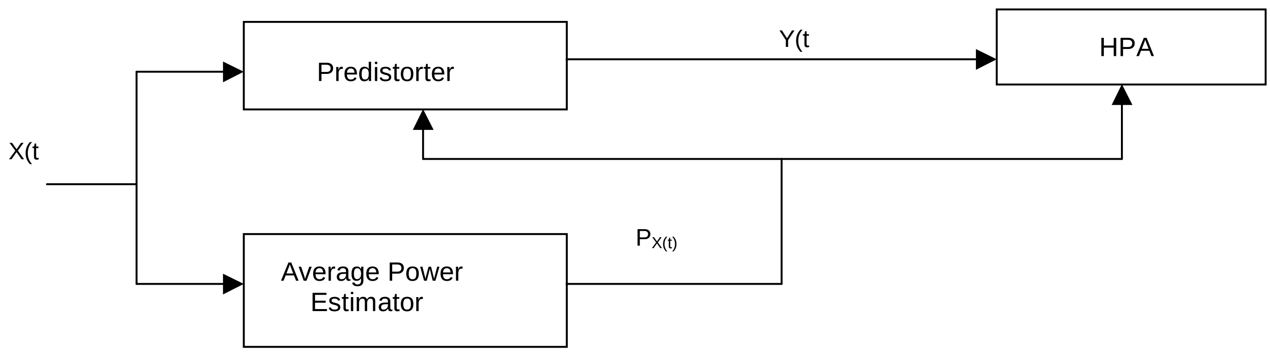

Using these characteristics, the complex signal Z(t) at the output of the HPA is very close to X(t), and the output power at the input saturation power of 0 dB is Δ dB less than its specified value. We have purposely introduced a loss of Δ dB in the AM-AM curve to reduce the clipping of the signal at saturation. Figure 10 illustrates this concept.

As in the linear-log model, the AM-AM/AM-PM look-up table for the PD, using this approach for the modified linear-log model, simply includes the P_{IN}(dB) versus $P_{PD\text{-}MOD}$(dB) curve for AM-AM and the P_{IN}(dBw) versus $\theta_{PD\text{-}MOD}$(degree) curve for AM-PM.

3. Implementation of the PD in Signal Processing Workstation (SPW)

Based on the models derived above and the block diagram shown in Figure 1(b), the implementation of the linearizer using PD circuit can be implemented in SPW as shown in Figure 1(c). The input signal X(t) is used to set the operating point for both the PD and HPA. This setting ensures one-to-one mapping between the PD and TWTA.

The simulation model for a typical HPA, e.g., TWTA, is shown in Figure 2. The approach shown in this figure uses look-up table to perform AM-AM and AM-PM conversion. The look-up table stores the measured data for a specified TWTA or SSPA. The operating point is set relative to the average power before the input power is used to find the corresponding gain and phase shift. A detail description for the implementation of HPA can be found in [6].

Figure 3 illustrates the implementation of the PD shown in Figure 1(c). This figure shows that the block diagram used in the HPA implementation can be reused with minor modifications for modeling the PD. The PD uses the same input X(t) to set the operating point as the HPA. Thus the operating point on the AM-AM and AM-PM curves are the same for PD and HPA. In using the linear-log model, the square-root of the normalized input signal is used to cancel out the effect of combining the two curves, namely, PD's AM-AM curve and HPA's AM-AM curve [see appendix].

4. Application to GBS

This section applies the PD algorithms derived in Section 2 to the TWTA actually used by the transponder onboard the GBS satellite. Figure 4 shows the measured normalized input voltage vs. output voltage of the TWTA. This figure also plots Eqn (3a) with the following values for the curve-fitting coefficients (see appendix): a_0 = 3.7407, b_0 = 0.3063, $\alpha_0 = 11.1163$, and β_0 = 4.2947. Figure 4 represents the AM-AM effects caused by the power amplifier operating at or near saturation.

Figure 5 shows the measured data for the TWTA input phase as a function of the normalized input voltage. This curve represents the AM-PM effects caused by the TWTA operating at saturation. This figure also plots Eqn (3b) with curve-fitting coefficient values: a_1 = 0.4978, b_1 = 0.1273, $\alpha_1 = 74.6172$, and β_1 = 1.0879.

Figure 2. Simulation Model for a typical High Power Amplifier in SPW

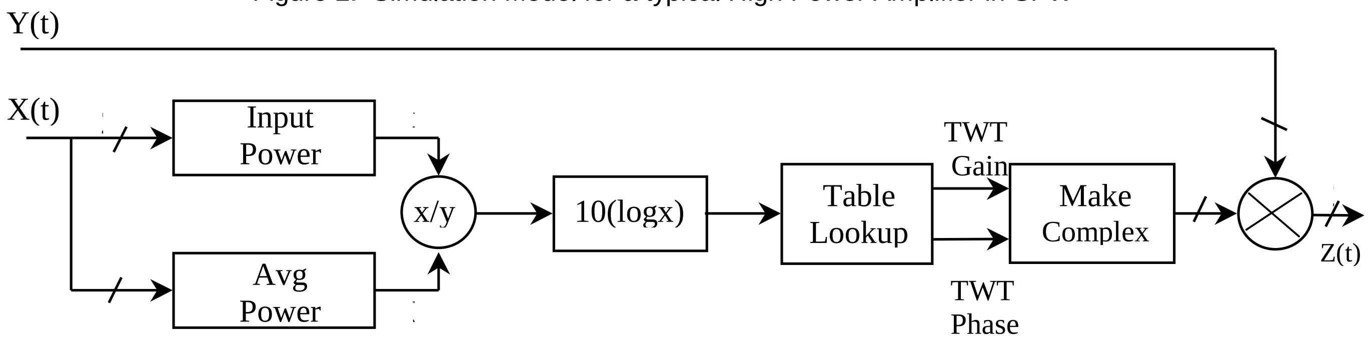

Figure 3. Simulation Model for a typical PD in SPW

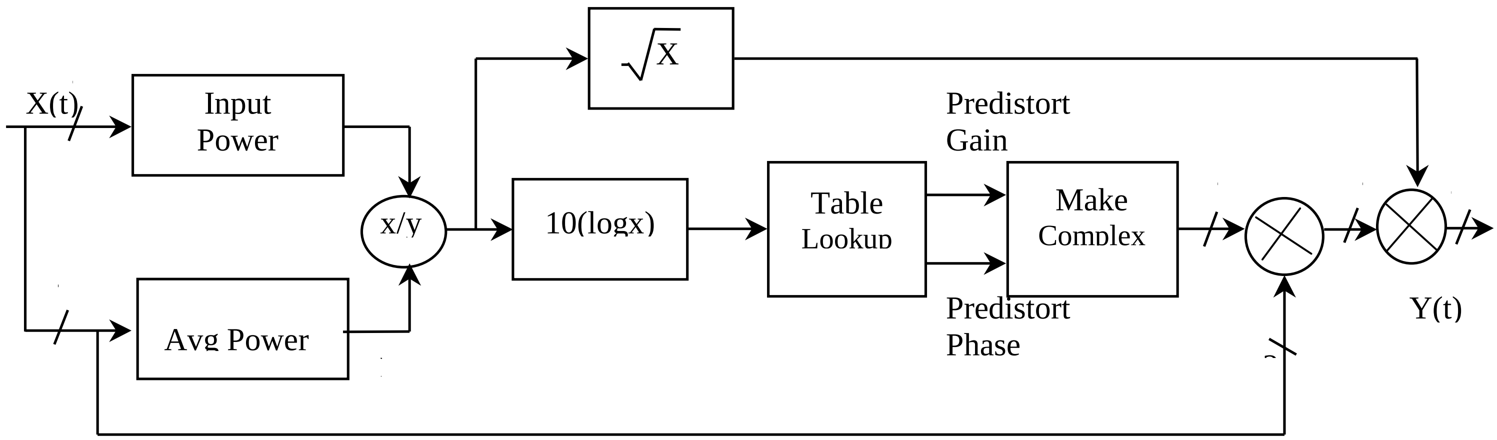

Figure 4. Normalized Output Voltage vs. Normalized Input Voltage for the GBS TWTA

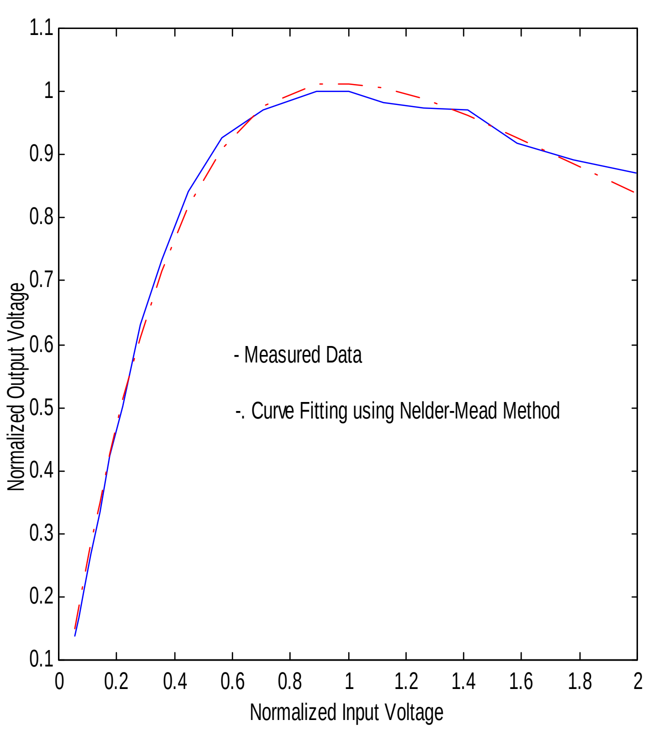

Figure 5. Output Phase vs. Normalized Input Voltage for the GBS TWTA

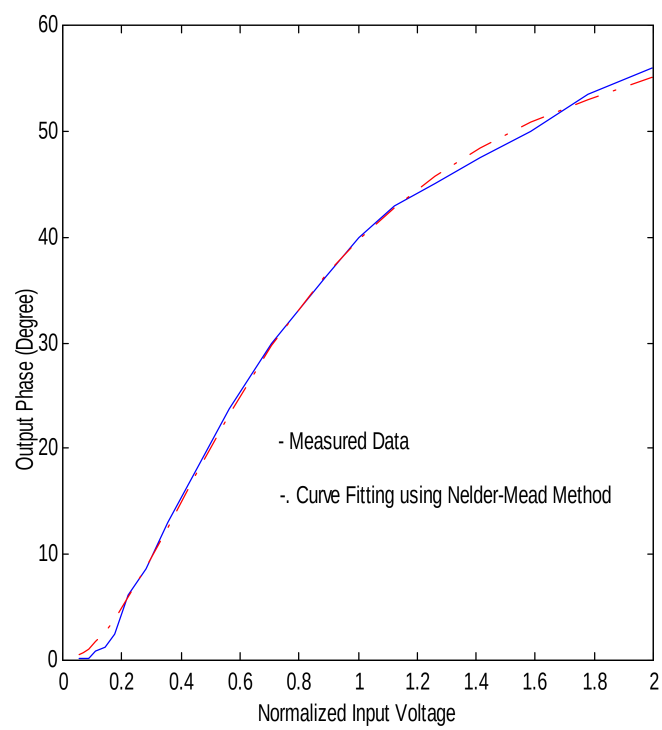

4.1 Implementation of Extended Saleh's Model

The extended Saleh's model derived in Section 2.2.1 allows us to characterize the PD. Using Eqns (11) and (12) with the curve-fitting coefficients found in Figures 4 and 5, we plot the amplitude and phase responses of the PD in Figures 6 and 7, respectively.

Figure 6. Input and Output Power Relationship of the PD Model Using Extension of Saleh's Model for the GBS TWTA

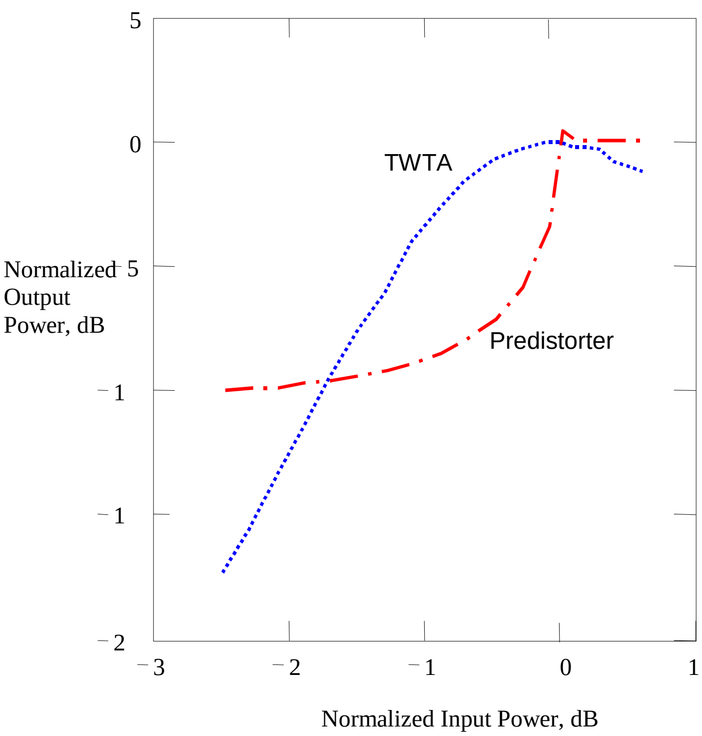

4.2 Implementation of Linear-Log Model

The linear-log model has been derived in the Appendix and described in Section 2.2.2. Using Eqns (13) and (15) with the measured data sets found in Figures 3 and 4, we plot the amplitude and phase responses of the PD in Figures 8 and 9, respectively.

Figure 7. Input and Output Phase Relationship of the PD Using Extension of Saleh's Model for the GBS TWTA

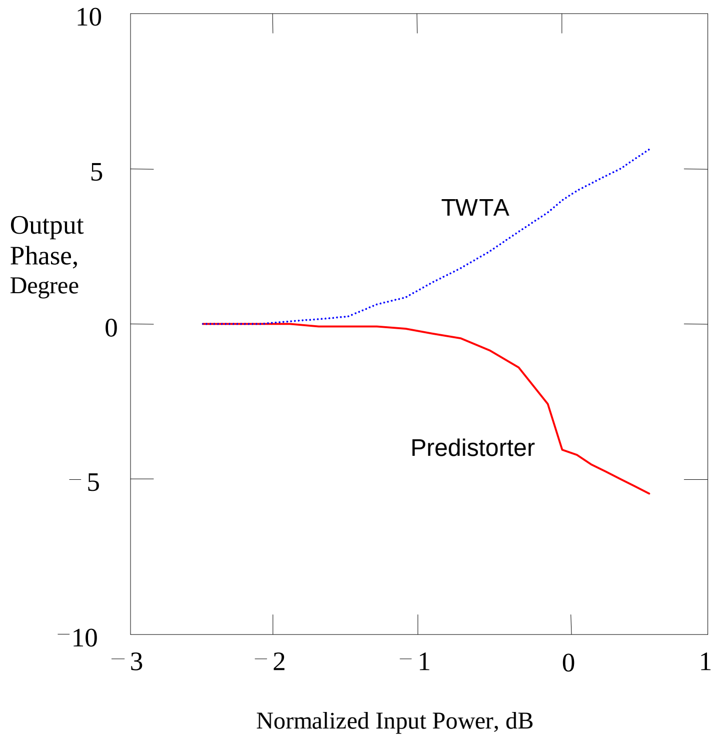

Figure 8. Input and Output Power Relationship of the PD Model Using Linear Log Model for the GBS TWTA

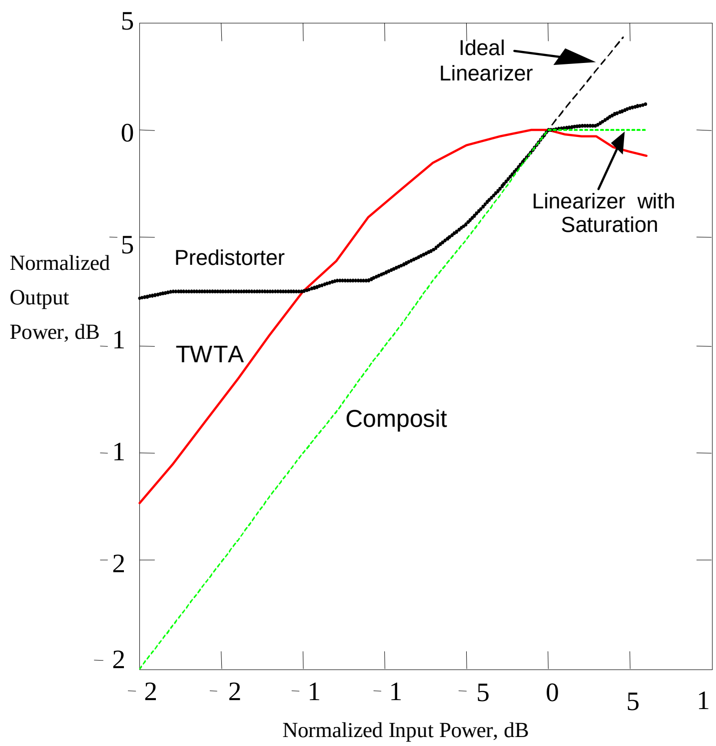

4.3 Implementation of Modified Linear-Log Model

The modified linear-log model has been described in Section 2.2.3. Using Eqns (17), (19) and (20) with the measured data sets found in Figure 3 and Δ(dB) = 1.0 dB, we plot the amplitude response of the PD in Figure 10. The phase response for the AM-PM is identical to the curves in Figure 9.

Figure 9. Input and Output Phase Relationship of the PD Using Linear Log Model for the GBS TWTA

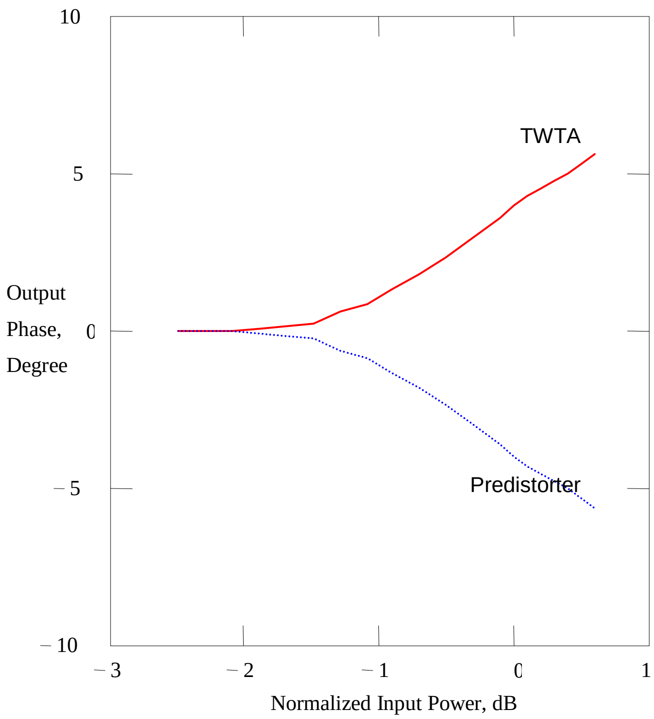

5. Numerical Results

A computer simulation based on the DVB modem and the GBS transponder implemented in SPW [7] has been created to evaluate the performance of the proposed linearizer using PD circuit. Using these SPW models we have evaluated the Power Spectral Density (PSD) and the Bit Error Rate (BER) performance of the DVB waveform with and without the PD. Figures 11(a) and (b) show the simulated DVB PSD at the input and output of the GBS transponder with and without the PD. These figures show that the use of the PD improves the bandwidth by more than twice of the symbol rate, and achieves almost 10 dB suppression of the second harmonic. These plots also show that the modified linear log models perform slightly better than the linear-log model (at the expense of power efficiency). In addition, Figure 11(a) also shows that the linearizer using the extended Saleh's model increases the occupied bandwidth.

Figure 10. Input and Output Power Relationship of the PD Model Using Modified Linear Log Model for the GBS TWTA

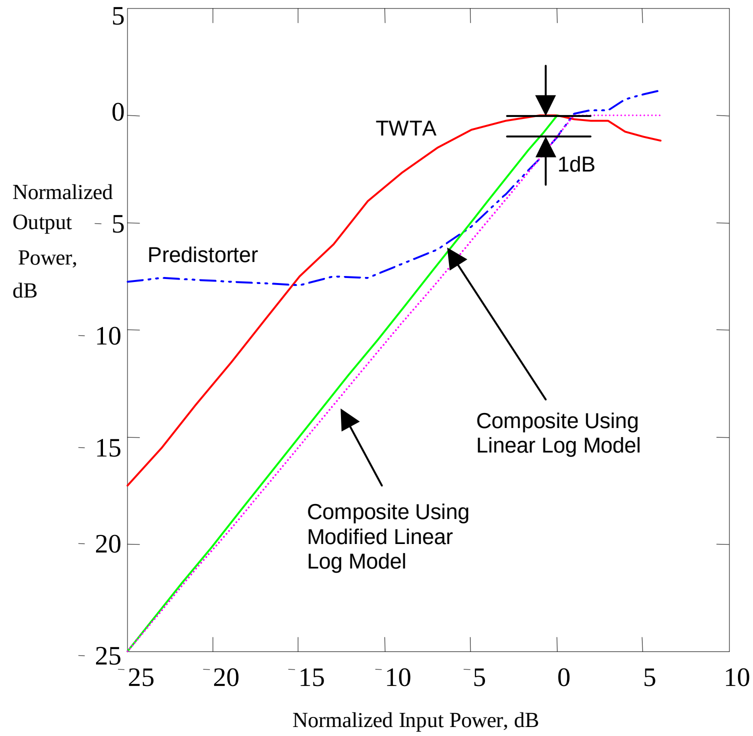

Figures 12(a) and (b) illustrate the uncoded DVB BER performance for various PD models. These figures show that the linear-log model improves the bit SNR over TWTA without PD by about 0.5 dB at BER = 10^{-2} and about 1 dB at BER = 10^{-3}. Figure 12(a) shows that the linear-log model outperforms the extended Saleh's model by about 0.1 dB. The linearizer using the modified linear-log model for Δ(dB) of 0.1 and 0.5 dB was simulated against the linear-log model. The results are shown in Figure 12(b). It was found that there was no significant improvement using the modified models. For Δ(dB) = 1.0 dB, the improvement is in the order of 0.1 dB at BER = 10^{-2}, and less than 0.1 dB for Δ(dB) = 0.5 dB

Figure 11. Power Spectral Density of DVB at the input and Output GBS Transponder With and Without Predistorter

(a) PSD for Linear-Log and Extended Saleh's Models

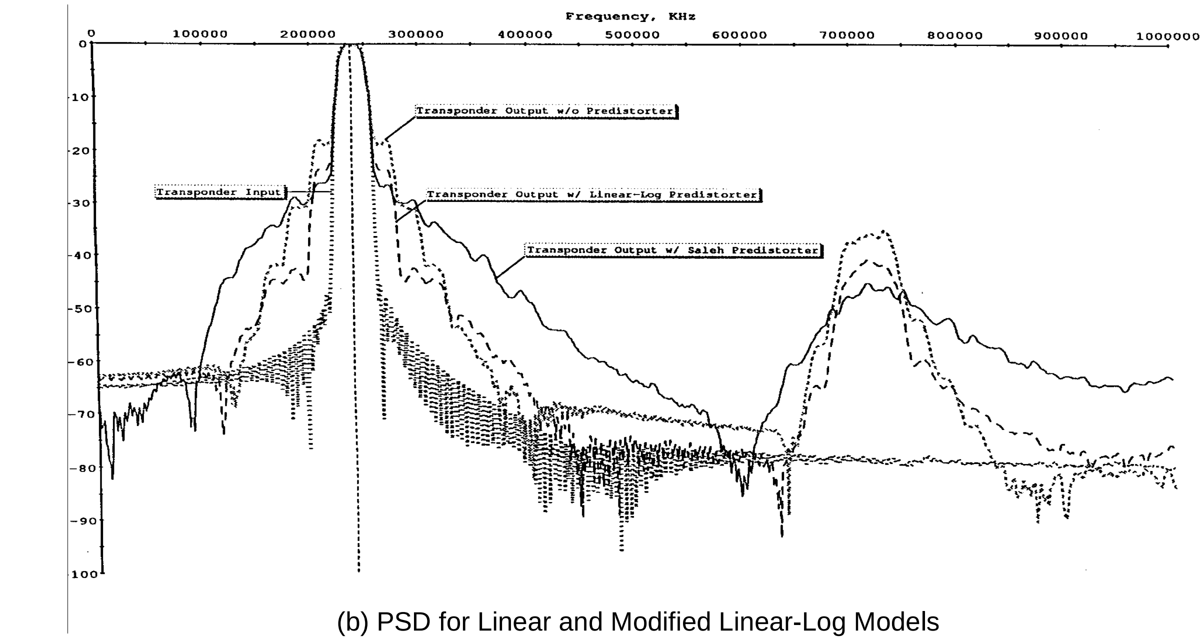

(b) PSD for Linear and Modified Linear-Log Models

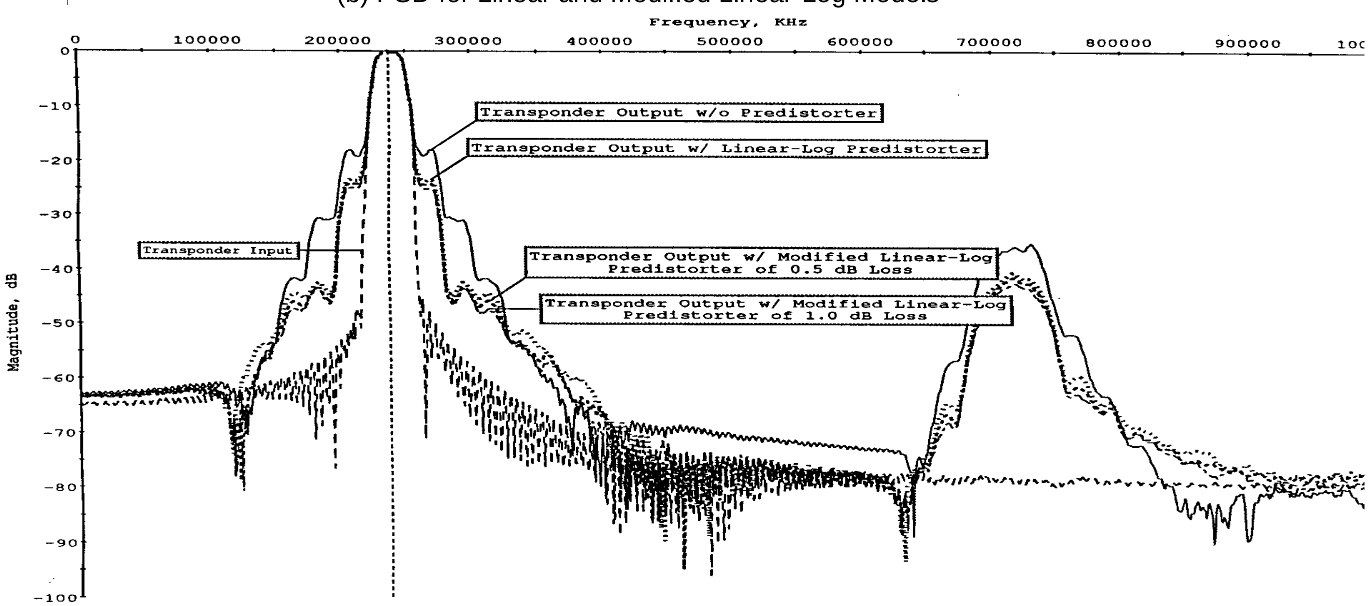

6. Conclusions

This paper has shown that the effects of the non-linear HPA can be compensated for by using PD circuit at baseband. The paper has proposed three models for the PD, namely, extended Saleh's model, linear-log model and modified linear-log models.

The extended saleh's model has slightly better out-of-band rejection performance than linear-log and modified linear-log models. But it requires a larger occupied bandwidth. The BER improvements for all models are about 0.5 db to 1.5 db depending on the BER. In addition, it has been shown that the extended Saleh's model has a closed-form solution, which requires much less memory than the look-up table approach; and furthermore, there is no need for interpolation. The closed-form solution for the extended Saleh's model allows it to be more flexible toward new or changed HPA parameters. However, the look-up table approach for linear-log and modified linear-log models are easier to derive from the HPA tables than the extended Saleh's model.

Figure 12(a). Uncoded DVB BER Performance for Linear-Log and Extended Saleh Linearizers

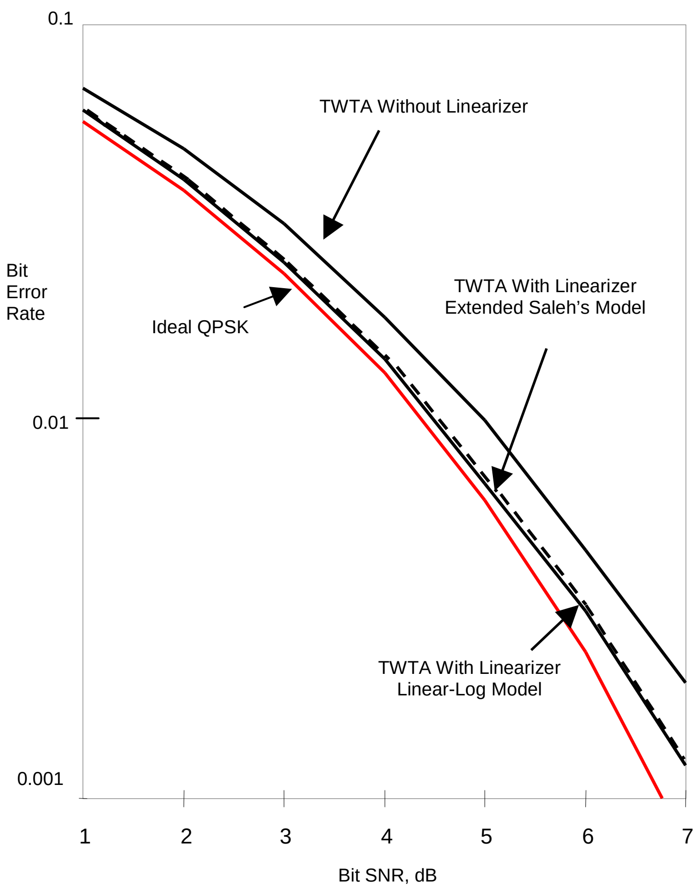

References

[1] Adel A. M. Saleh, "Frequency-Independent and Frequency-Dependent Nonlinear Models of TWT Amplifiers," IEEE Transactions on Communications, Vol. Com-29, No. 11, November 1981.

[2] Osamu Shimbo, "Effects of Intermodulation, AM-PM Conversion, and Additive Noise in Multicarrier TWT Systems," Proceedings of the IEEE, Vol. 59, No. 2, February 1971.

Figure 12(b). Uncoded DVB BER Performance for Linear-Log and Modified Linear-Log Linearizers

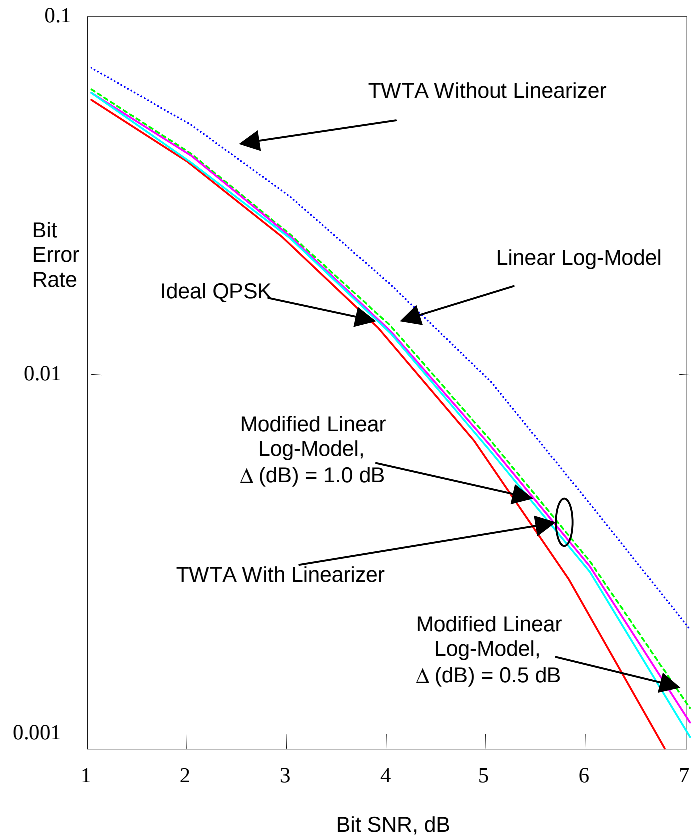

[3] J. C. FuenZalida, O. Shimbo, and W. L. Cook, "Time Domain Analysis of Intermodulation Effects Caused by Non-Linear Amplifiers," COMSAT Technical Review, Vol. 3, No. 2, Spring 1973.

[4] Aldo N. Andrea, Vincenzo Lottici, and Ruggero Reggiannini, "RF Power Amplifier Linearization Through Amplitude and Phase Predistortion," IEEE Transactions on Communications, Vol. 44, No. 11, November 1996.

[5] John M. Charroux, Tien M. Nguyen, Michael Thorburn and Herbert J. Wintroub, "Impact of the Non-Linear Amplifier on the Combined GMSK Signals," to be published in the Proceedings of MILCOM'98.

[6] Alta Group of Cadence Design Systetms, Inc., “Signal Processing WorkSystem-Communications Library Reference, “ Product No.: COM8000, June 1994.

[7] Tien M. Nguyen, James Yoh, et. al, “Performance Evaluation of the DVB and DSS Waveforms for Blobal Broadcast Services-Part I: Baseline Model with Perfect Components,” Aerospace Report No. TOR-98-1464-1, June 1998, The Aerospace Corporation, El Segundo, California.

[8] J.A. Nelder and R. Mead, “A Simplex Method for Function Minimization”, Comput. J., 7, pp. 308-313, 1965.

Acknowledgement

The authors would like to thank Dr. Gee Lui and Dr. Keith SooHoo for their useful comments and suggestions to improve the writing of this paper and John Charroux for his assistance in SPW.

APPENDIX I

The Parameter Estimation Problem

In this section, we consider the problem of estimation of coefficients $q_{AM} = (a_0,\ \mathrm{b}_0,\ \alpha_0,\ \beta_0)$ and $q_{PM} = (a_1,\ \mathrm{b}_1,\ \alpha_1,\ \beta_1)$ given measured data of the Eqns (3a) and (3b). That is, given measured data $M^d(\rho_{y(t_i)})$ for AM-AM response of the HPA at time t_i, $i = 1,2,\ldots,N$ we seek to determine a best estimate $\hat{q}_{AM}$ that minimizes a least squares criterion

$$J(q_{AM}) = \sum_{i=1}^{N} | M(\rho_{y(t_i)}, q_{AM}) - M^d(\rho_{y_i(t)})|^2 , \qquad \text{(AI.1)}$$

where $M(\rho_{y(t_i)}, q_{AM})$ is the normalized AM-AM response of the HPA due to the input signal $Y(t_i)$ at each time t_i, $i = 1,2,\ldots,N$ corresponding to the parameter set q_{AM}, Eqn (3a). The parameter estimation problem for the parameter set q_{PM} can also be formulated similarly.

The above optimization problem is an unconstrained minimization problem. The method used to obtain the solution to this minimization problem is based on function information computed on sequences of simplices and is known as the Nelder-Mead algorithm [8]. Basically, given the optimization problem

$$\min_{q \in \mathrm{R}^n} J(q) \qquad \text{(AI.2)}$$

(in our case, $q = q_{AM}$ or $q_{PM} \in R^4$), the Nelder-Mead algorithm maintains a simplex of approximations to an optimal point. We assume throughout that the vertices $\{q_j\}_{j=1}^{n+1}$ are sorted according to the objective function values (AI.3)

$$J(q_1) \le J(q_2) \le \ldots \le J(q_{n+1}).$$

The point q_1 is referred to as the best vertex and q_{n+1} is the worst vertex. The algorithm attempts to change the worst vertex q_{n+1} to a new point by the formula

$$q(\delta) = (1+\delta)\bar{q} - \delta q_{n+1}. \qquad \text{(AI.4)}$$

Here, $\bar{q}$ is the centroid of the convex hull of $\{q_j\}_{j=1}^{n+1}$. More specifically, we compute $\bar{q}$ by the formula

$$\bar{q} = \frac{1}{n}\sum_{i=1}^{n} q_i . \qquad \text{(AI.5)}$$

The typical value for the parameter δ is

$$\delta = \{\delta_r, \delta_e, \delta_r, \delta_e\} = \{1,2,0.5,-0.5\} \qquad \text{(AI.6)}$$

which corresponds to the reflection, expansion, outside contraction, and inside contraction steps of the Nelder-Mead iteration. Figure 13 describes these steps for the case where the parameter set $\{q\}$ is in R^2.

The algorithm will terminate when either $J(q_1) - J(q_{n+1})$ is sufficiently small in absolute value or the number of function evaluations is larger than a user-prescribed value. In our calculations, we employed the Nelder-Mead simplex search algorithm *fmins* implemented in Matlab. The optimal sets of parameters, which gave the best least squares fit to the HPA measured data are given by

$$q_{AM} = \{3.6407, 0.3063, 11.1163, 4.2947\} \quad \text{(AI.7)}$$

$$q_{PM} = \{0.4978, 0.1273, 74.6172, 1.0879\} \quad \text{(AI.8)}$$

Figure A.1. Nelder-Mead Simplex and New Points

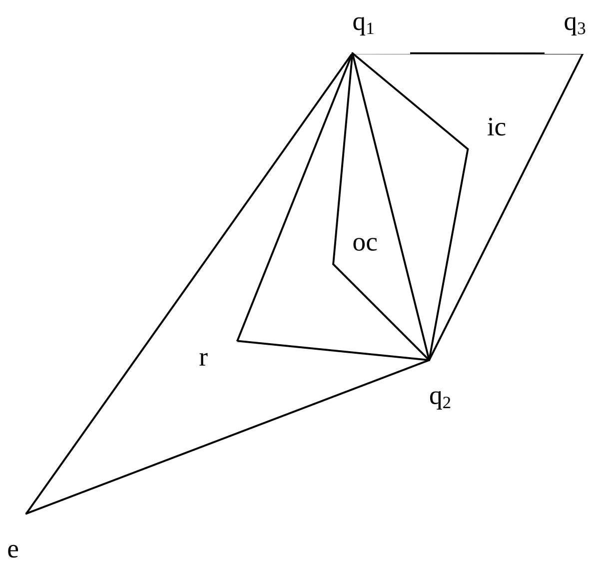

Figures 4 and 5 depicts the graphs of the normalized output voltage and output phase respectively as computed using the least squares fit parameters plotted against the measured data. These graphs show a very good agreement between the measured data and the model.

APPENDIX II

Derivation of Linear-Log Model

A simplfied block diagram for the linearizer is shown in Figure 1(c). The first circuit is the predistorter circuit, followed by the HPA circuit. A third circuit provides for the average input power, $P_{x(t)}$, that is constantly being updated. The intent of the predistorter circuit is to distort its input, X(t), in such a way that the output of the HPA circuit, Z(t), will be exactly equal to X(t) at every instant.

The predistorter circuit is shown in Figure 3. The two inputs to the circuit are X(t) and $P_{x(t)}$. Tracing the lower path, the input to and output from the block AM_AM AM_PM TABLE_LOOKUP for the predistorter are given by:

Input power: $P_{IN}(dB) = (\rho_{x(t)}^2/P_{x(t)})_{dB}$ (AII.1a)

Output power: $P_{PD}(dB) - P_{IN}(dB)$ (AII.1b)

Output phase: θ_{PD}(degree) (AII.1c)

where P_{PD}(dB) and θ_{PD}(degree) are the normalized output power in dB and output phase in degree obtained from the PD lookup table. Tracing through the rest of the circuitry, the output from the PD can be expressed as:

$$Y(t) = X(t)\sqrt{P_{PD}}\, e^{j\theta PD}\,(\deg ree) \quad \text{(AII.2)}$$

where P_{PD} is the normalized output power of the PD. This is the instantaneous output of the PD circuit in response to the input X(t).

The HPA circuit is shown in Figure 2. There are three inputs: X(t), $P_{x(t)}$ and Y(t). The lower path is identical to that of the PD circuit (Figure 3), except that the block AM_AM AM_PM TABLE_LOOKUP employs a table applicable to the HPA instead of the PD. The input and output of the block are given by:

Input power: P_{IN}(dB) (AII.3a)

Output power: $P_{HPA}(dB) – P_{IN}(dB)$ (AII.3b)

Output phase: θ_{HPA}(degree) (AII.3c)

where P_{HPA}(dB) and θ_{HPA}(degree) are the normalized output power in dB and output phase in degree obtained from the HPA lookup table. Tracing though the rest of the circuitry, the output from the HPA can be expressed as:

$$Z(t) = X(t)\sqrt{\frac{P_{HPA}}{P_{IN}}}\, e^{j\theta HPA}\,(\deg ree) \quad \text{(AII.4)}$$

where P_{IN} and P_{HPA} are the normalized input and output power of the HPA.

Substituting the expression in Eqn.(AII.2) for Y(t):

$$Z(t) = X(t)\sqrt{\frac{P_{PD}P_{HPA}}{P_{IN}}}e^{j[\theta_{PD}(\text{degree})+\theta_{HPA}(\text{degree})]}$$

(AII.5)

This is the instantaneous response of the HPA circuit to the PD input x(t).

In order to allow Z(t) and X(t) to be equal, the following relationships between the PD and HPA look-up tables must be maintained:

θ_{PD}(degree) = - θ_{HPA}(degree) (AII.6a)

$P_{PD}\ P_{TWTA} = P_{IN} = \rho_{x(t)}^2/P_{x(t)}$ (AII.6b)

With these relationships, the PD lookup table can be readily generated from the HPA look-up table. The first relationship requires that the phase distortion of the PD must be the negative of the phase distortion of the HPA. The second relationship requires that the combined magnitude gain of the PD and HPA lookup tables is unity. This relationship can be rewritten as:

P_{PD}(dB) = P_{IN}(dB) - P_{HPA}(dB) (AII.7)

If there were no limit to the output power from the HPA, the above treatment would give us a perfect linearizer, resulting in an output that is equal to the input at every instant of time. Unfortunately, this is not the case. The effect of HPA saturation must be modeled. With saturation, the best linearizer that can be achieved is clipped at saturation, as shown by the dotted curve in Figure 8. Eqn.(AII.6) produces the ideal linearizer response as indicated by the dashed curve in Figure 8. To obtain the linearizer response curve with saturation, Eqn.(AII.7) must be modified as follows:

P_{PD}(dB) = -P_{HPA}(dB) for P_{IN}(dB) > 0 dB (AII.8)

where it is assumed that the normalized input saturation power is at 0 dB. Eqn (AII.8) produces the clipped portion of the dotted curve in Figure 8.